Truncation Error in Image Interpolation

Loic Simon
GREYC CNRS UMR 6072
Ecole Nationale Supérieure d'Ingénieurs de Caen
Email:loic.simon@ensicaen.fr

***Abstract*—Interpolation is a fundamental issue in image processing. In this short paper, we communicate ongoing results concerning the accuracy of two landmark approaches: the Shannon expansion and the Discrete Fourier Transform (DFT) interpolation. Among all sources of error, we focus on the impact of spatial truncation. Our estimations are expressed in the form of upper bounds on the Root Mean Squared Error as a function of the distance to the image border. The quality of these bounds is appraised through experiments driven on natural images.**

I. Introduction

Regardless of their very digital nature, images must often be considered continuous. To some extent that we shall discuss, this conceptual "equivalence" is justified by the Shannon-Whittaker theorem. By any means, it is paramount for any application of image processing where sub-pixel operations are performed (such as in optical flow or stereopsis).

However fundamental, the Shannon-Whittaker theorem is by nature deceptive when considering practical circumstances for digital signals are noisy, possibly aliased and more importantly finite. As a result, any practical continuous reconstruction of such signals will be flawed. Among other error sources, one can list photon counting, quantization, aliasing and spatial truncation ([1]). The first three can be harnessed by different means. Photon counting noise can be lowered by increasing the exposure time, while quantization and aliasing are well controlled in recent High Dynamic Range (HDR) cameras.

On the contrary, the last source of error will prove to be much more troublesome. It is indeed the main goal of these notes to alert the readers on this issue. We will also give evidence that this is especially true for images, due to their relatively narrow spatial extension and to their slow spectral decay (mainly when textures are present).

It is rather awkward that the truncation error is often entirely ignored in image processing. It was nonetheless studied in other communities of signal processing. This is for example the case of [2], [3], [4] and [5]. These articles are all dedicated to the truncation error. They include upper bounds valid under diverse circumstances. Unfortunately, because they were developed in different contexts, these results are not so well adapted to images.

In [2] for instance, the signal is assumed bounded. This is certainly true for images since they are encoded on the range between 0 and 255. However in practice their bound yields a large overestimation because its tightness is proportional to the signal dynamic which often exceeds greatly the signal local variability. In [3], [5] the signal is assumed over-sampled, a case often referred to as the guard band assumption in the literature. Such an assumption may be realistic for audio signals but not for images. Note that in the limit where the guard band vanishes, the upper bounds explode inescapably.

While standing no exception to the previous limitations, the study presented in [6] has yet been very inspirational. It considers signals as stationary random processes and proposes two upper-bounds depending upon whether the signal is over-sampled or not. If not, the upper-bound is proportional to the maximum value of the spectrum. This maximum value is generally large and does not lead to a practical upper-bound.

Let us mention also [7], where the problem of Shannon-Whittaker interpolation is directly posed for duration-limited signals. Instead of considering convergence upon an infinite number of samples, the authors let the sampling rate tend to infinity. As a result, no band-limited assumption is required on the signal. The counterpart is that upper bounds are derived and expressed in term of the modulus of continuity of the signal. Such a property can only be known in certain application domains, and certainly not in classical image processing.

All the articles we have mentioned so far concentrate on the Shannon expansion, while in practice, the DFT interpolation is preferred due to a lesser time complexity. To our knowledge, upper-bounds in that case have only been studied in [8]. Their approach is similar to [3] and hence suffers the same limitations. Since the DFT interpolation is equivalent to the exact Shannon expansion under periodic conditions, a periodic plus smooth decomposition [9] may improve its performance.

It is worth noting that the general study of interpolation error can be considered a sub-field of approximation theory. One fundamental and quite powerful result, known as the Strang-Fix conditions [10], relates the capability of a linear shift invariant approximation system to its order of approximation. It was for instance used by Blu et al. (see [11]) to estimate spline based approximation errors. One should note however that these developments concern shift-invariant (and thus infinite) sampling grids. As a result they do not apply to the truncation error. Moreover, it was shown in [12] that in this context at least, the most accurate approximation methods are not interpolating. In a nut shell, imposing a perfect reconstruction of the signal at the sampling position has a negative effect on the overall reconstruction.

For what concerns us, we shall concentrate our efforts on the truncation error and endeavour to obtain realistic estimations of the actual error. Due to lack of space, results shall be presented in a summarized way (*e.g.* without proof and using

the Landau notation). Further details (proofs and tightness analysis) will be included in a forthcoming publication.

II. Notations and Assumptions

In what follows, X_t stands for a random process (RP), where $t \in \mathbb{R}$ might be either a time or space variable. The Fourier transform of a deterministic signal x_t will be denoted by $\mathcal{F}(x)$ and defined as $\mathcal{F}(x)(\omega) := \frac{1}{2\pi}\int e^{i\omega t}x_t dt$.

All RPs are assumed weakly stationary, in other terms with time-invariant first and second order statistics. For such a process X_t, we will generically denote by $\mu := \mathbb{E}[X_t]$ its average, by $R_X(t) := \mathbb{E}[(X_\tau - \mu)(X_{\tau+t} - \mu)]$ its auto-correlation function and by $d\Psi_X(\omega) := \mathcal{F}(R_X)(\omega)$ its power spectral distribution. All RPs are further assumed strictly Nyquist band-limited, which is to say that $d\Psi_X(\{|\omega| \geq \pi\}) = 0$.

Given a RP X_t, we will denote by $X.\Delta_K := \sum_{|k|\leq K} X_k \delta_k$ the sampled version on the finite grid $\{k \in \mathbb{Z}, |k| \leq K\}$. For a fixed $K > 0$, the number of samples will always be denoted by $N = 2K+1$. We consider linear shift-invariant reconstructions from such a sampled version in the form

$$[(X.\Delta_K) * h_K](t) = \sum_{|k|\leq K} X_k h_K(t-k),$$

where $h_K(t)$ is any function referred to as a reconstruction kernel. In this article, we will mainly consider two examples,

- the Shannon kernel $\mathrm{sinc}(t) := \frac{\sin(\pi t)}{\pi t}$ and
- the DFT (or Dirichlet) kernel $\mathrm{sincd}[K](t) := \frac{\sin(\pi t)}{N\sin(\frac{\pi t}{N})}$.

A. Goal

We will appraise the quality of a given reconstruction based on the Root Mean Squared Error (RMSE),

$$RMSE_{[X,h_K]}(t)^2 := \mathbb{E}\left[\left(X_t - [(X.\Delta_K) * h_K](t)\right)^2\right].$$

Resting upon intuitive observations, we shall highlight two predictable features of the RMSE. First, since any interpolation is supposed to perform perfectly at the sampling locations, the RMSE is likely to oscillate, being null at any sample and maximal approximately midway between successive samples. Besides, a RP can be theoretically recovered through the Shannon expansion, if sampled on an infinite grid. Therefore, we expect the error to be tied to the lack of knowledge outside the finite sampling domain, and as such to diminish as we move farther away from the borders. Accordingly, our goal consists in evaluating the decay (up to an oscillating modulation) of the RMSE as the distance varies. We set

$$\delta(t) := \min(K + \frac{1}{2} - t, K + \frac{1}{2} + t). \tag{1}$$

III. Theoretical RMSE bounds

Theorem 1 (Spectral representation of the RMSE): Let X_t be a RP of average μ and power spectrum $d\Psi_X$, $K < \infty$ and h_K a reconstruction system. Then,

$$RMSE_{[X,h_K]}(t)^2 = MSE_{\mu,h_K}(t) + MSE_{d\Psi_X,h_K}(t),$$

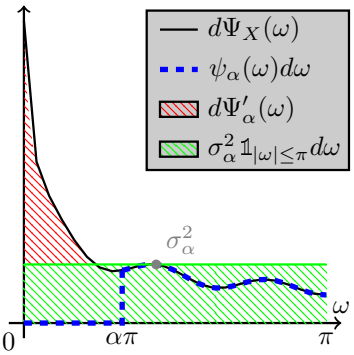

Fig. 1. The spectrum decomposition of Proposition 2.

where

$$MSE_{\mu,h_K}(t) := \mu^2 \left|1 - \Delta_K * h_K(t)\right|^2,$$
$$MSE_{d\Psi,h_K}(t) := \frac{1}{2\pi}\int \left|e^{i\omega t} - [(e^{i\omega\cdot}\Delta_K) * h_K](t)\right|^2 d\Psi(\omega).$$

This theorem merely states that the mean squared error is the sum of the squared errors with respect to the average value of X and with respect to every pure harmonic $e^{i\omega t}$ (weighted by the spectrum of X). The conclusion holds true even if X_t is not band-limited and under mild assumptions (applying to a sequence of h_K's) when $K \to \infty$.

We shall need to evaluate the behavior of each component of the previous decomposition. We refer to them respectively as the average MSE component and the power spectral MSE component. Unlike the previous theorem, the next proposition is specific to strictly Nyquist band-limited RPs.

Proposition 1:

$$MSE_{\mu,h_K}(t) = \mu^2 \left|[\Delta_\infty * \mathrm{sinc}](t) - [\Delta_K * h_K](t)\right|^2,$$
$$MSE_{d\Psi_X,h_K}(t) = \frac{1}{2\pi}\int_{|\omega|\leq\pi} d\Psi_X(\omega) \times \left|[(e^{i\omega\cdot}\Delta_\infty) * \mathrm{sinc}](t) - [(e^{i\omega\cdot}\Delta_K) * h_K](t)\right|^2.$$

Building upon existing works and the analysis of their flaws with respect to specific spectrum characteristics of images, we propose an essential step to obtain realistic bounds. The trick resides in decoupling the low frequencies of the spectrum from a residual component equivalent to band-limited white noise. This process, illustrated in Figure 1, results in

Proposition 2 (Spectrum decomposition): Let $0 \leq \alpha < 1$ and assume that $\mathbb{1}_{|\omega|\geq\alpha\pi} d\Psi_X(\omega) = \psi_\alpha(\omega)d\omega$, with $\psi_\alpha(\omega) \leq \sigma_\alpha^2$. And let $d\Psi'_\alpha$ the positive component of $d\Psi_X - \sigma_\alpha^2 d\omega$. Then,

$$MSE_{d\Psi_X,h_K}(t) \leq MSE_{d\Psi'_\alpha,h_K}(t) + \sigma_\alpha^2 MSE_{\mathbb{1}_{|\omega|\leq\pi}d\omega,h_K}(t).$$

In the previous statement, the first term in the right-hand-side corresponds to an over-sampled signal and the second one to the aforementioned residual band-limited white-noise. In addition, α can be set freely; a freedom we shall exploit to tighten the RMSE bounds which follow.

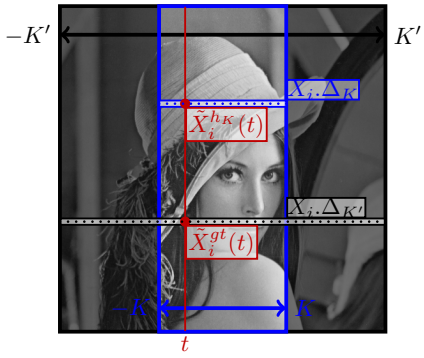

Fig. 2. Construction of the RMSE and spectrum estimators. Interpolation is conducted along the x-axis and averaging along the y-axis.

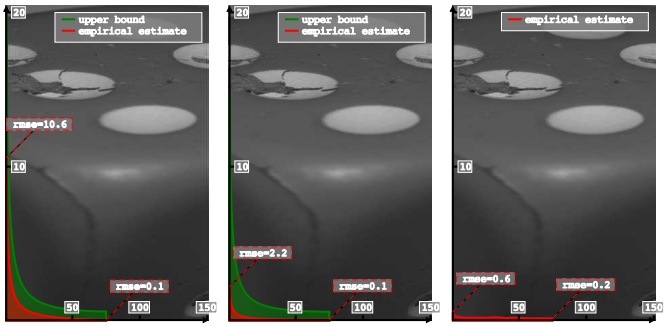

(a) Shannon (b) DFT (c) B-spline 9

Fig. 3. RMSE estimator and upper bound for the dice image.

Theorem 2: Under the same assumptions and notations as in Proposition 2, and with the kernel h_K associated with either the Shannon expansion or the DFT interpolation, we have

$$RMSE_{[X.\Delta_K * h_K]}(t)^2 = \frac{\sin^2(\pi t)}{\pi^2} \times \begin{pmatrix} \mu_X^2 \mathcal{O}\left(\frac{1}{\delta(t)^2}\right) \\ + \\ {\sigma'}_\alpha^2 \mathcal{O}\left(\frac{1}{\delta(t)^2}\right) \\ + \\ \sigma_\alpha^2 \mathcal{O}\left(\frac{1}{\delta(t)}\right) \end{pmatrix},$$

where

$${\sigma'}_\alpha^2 := \frac{1}{2\pi} \int_{|\omega| \leq \alpha\pi} \frac{2}{1+\cos(\omega)} d{\Psi'}_\alpha(\omega).$$

This provides a decomposition of the mean squared error into a **modulation** times an **envelope**. Following the previous developments, the latter has been decomposed into three terms referred as the **average** envelope, the **low-frequency** envelope and the **white-noise** envelope. This decomposition is valid for the two aforementioned interpolation methods. However the domination constants are different. Precisely, in the DFT, the average envelop is null while the remaining two constants are twice as large as those of the Shannon case.

IV. Experimental settings

In order to scrutinize the correctness of our upper bounds and determine how insightful the information they provide, we have designed an experimental framework[1]. Aspiring to provide practical conclusions on natural images, we could not resort to synthetic signals for which we could have obtained closed-form expressions of the quantities of interest. Instead, given an image exemplar and an interpolation method, our goal would be to estimate the RMSE bound as well as an accurate approximation of the RMSE at varying distances. As illustrated in Figure 2, we will perform interpolation along the horizontal dimension and take advantage of the remaining dimension to perform empirical averages when needed.

The upper bound calculation relies on the image average and two spectral statistics: σ_α and σ'_α. Assuming the spectrum to be absolutely continuous, its density verifies $\psi_X(\omega) = \mathbb{E}\left[|\mathcal{F}(X)(\omega)|\right]^2$. It can thus be estimated at discrete frequencies as an average $\psi_X(\omega_k) \simeq \frac{1}{M}\sum_{i=1}^M |\mathcal{DFT}(X_i)|^2(\omega_k)$.

Assuming that we knew the signal at a given location t, the RMSE could be approached by

$$RMSE^2_{X,h_k}(t) \simeq \frac{1}{M}\sum_{i=1}^M (X_{i,t} - \tilde{X}_{i,t}^{h_K})^2,$$

where to shorten notations $\tilde{X}_{i,t}^{h_K} := [(X_{i,.}\Delta_K) * h_K](t)$. The only challenge here relates to the estimation of the ground-truth interpolated signal. A simple idea would be to subsample an input image, and re-interpolate it with the method under consideration at the missing samples. Obtaining the ground-truth could not be more straightforward. However this scheme does not fulfil other requirements, especially since it violates the Nyquist band-limited assumption.

Instead, as illustrated in Figure 2, starting from an image of half-width K', we restrict the evaluation to a central sub-image of half-width K. That is to say, we apply the interpolation method under test based on this subset of the samples and obtain interpolated samples $\tilde{X}_{i,t}^{h_K}$ in a super-grid of the central region $t \in \{-K, -K+dt, \ldots, K\}$. We then use the whole image to compute (pseudo-)ground-truth samples $\tilde{X}_{i,t}^{gt}$ at the same locations thanks to the Shannon expansion.

We must point out that the previous strategy has one major drawback. Indeed, since we wish the ground-truth to be much more accurate than the considered interpolation, the margin between the whole image borders and the central region must be large compared to the central extent, *i.e.* $K' \gg K$. Besides, the errors made in $\tilde{X}_{i,t}^{gt}$ and $\tilde{X}_{i,t}^{h_K}$ are due to missing samples, a majority of which are shared. Therefore these errors are correlated and result in a negative bias of the RMSE estimator.

V. Experimental results

Here we present the results on two images. For each image, we plot the RMSE estimator for the Shannon expansion, the DFT and the 9^{th}-order b-spline interpolation, as well as the theoretical upper bound when available.

The two images were chosen to illustrate opposite behaviours associated with different spectral contents. Indeed, the first image (Figure 3) is very smooth whereas the second

[1] Available at http://dev.ipol.im/~simonl/ipol_demo/loic_truncate.

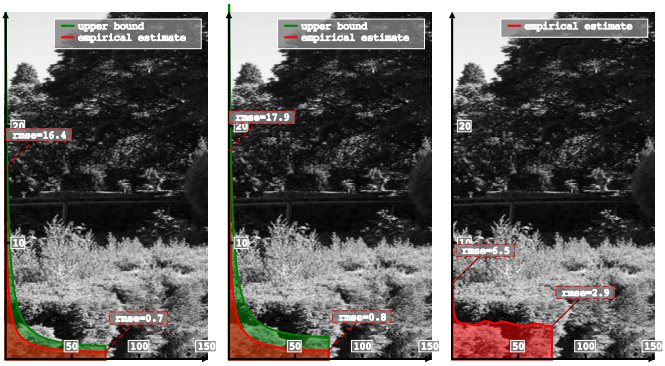

(a) Shannon (b) DFT (c) B-spline 9

Fig. 4. RMSE estimator and upper bound for the garden image.

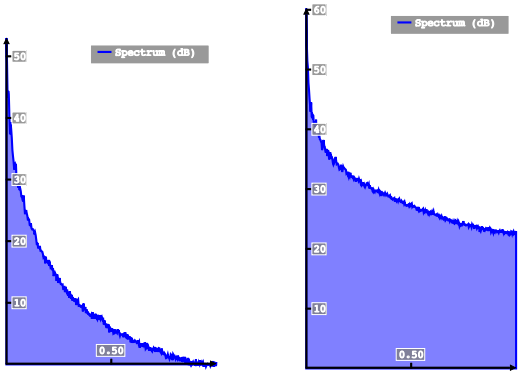

(a) Dice (b) Garden

Fig. 5. Comparison of the spectra in dB for the dice and the garden image.

one (Figure 4) presents various textured regions. We should then expect the white-noise component to be more important in the second case. To confirm this, a visual comparison of the estimated spectra is depicted in Figure 5. In both cases, the upper bound is consistent with the estimator. One cannot fail to observe that the gap between the two curves is greater in the smooth case. This might be explain either by a stronger bias in the estimator or by a lesser sharpness of the upper bound. In any case, consistently with our prediction, the worst-case scenario occurs with highly textured images. It is therefore a great achievement to ensure as tight an estimation in this case. In fact, we have obtained closed-form expressions of the tightness (for white-noise) that confirm our doing so.

Studying closely the values in Figure 4 reveals that for a 150 pixels wide and highly textured image, the interpolation error might very well exceed the quantization (whose RMSE amounts to 0.29) everywhere. The decay of the RMSE as the square root of the inverse distance is then extremely problematic, since it means that to achieve a 2fold decrease of the RMSE the distances must be multiplied by 4. This point brings out dramatic conclusions when considering 16-bits HDR images. Practically, it means that for the same level of accuracy (relatively to the quantization RMSE) the distances must be multiplied by 256^2.

Considering the comparison between the Shannon/DFT methods and B-splines, the most noticeable difference concerns the shape of the RMSE curve. The B-splines error decreases much more quickly and flattens. Unfortunately, the attained value is much larger than in the other methods.

VI. Conclusion

We have presented ongoing results concerning a systematic error which occurs in interpolation. Although similar studies have been published in the past, their knowledge does not seem widely spread among the image processing scientists. More importantly, their applicability to natural images is limited. On the contrary, our study is motivated by practical needs in image processing and is therefore directed toward this specific context. In particular, from the start we took into consideration the possible presence of smooth regions as well as textures.

After presenting the main steps to the theoretical upper bound, we have described an experimental framework and some selected results. A consensus emerged among theoretical and experimental conclusions wherein textured images proved to be a worst-case scenario. The relatively slow decay of the RMSE in that case appears as a major obstacle to highly accurate image processing.

We hope that this paper sheds new light on the legitimacy of the conceptual equivalence of digital and continuous images. It should as well provide a sound starting point to consider accuracy estimations in sub-pixel image processing applications. We do plan to explore such path in the near future.

Acknowledgment

The author would like to thank Jean-Michel Morel for bringing this topic to his attention and the anonymous reviewers for their fruitful suggestions.

References

[1] A. J. Jerri, "The Shannon sampling theorem - its various extensions and applications; a tutorial review," *Proceedings of the IEEE*, vol. 65, 1977.
[2] D. Jagerman, "Bounds for truncation error of the sampling expansion," *SIAM Journal on Applied Mathematics*, vol. 14, 1966.
[3] K. Yao and J. B. Thomas, "On truncation error bounds for sampling representations of band-limited signals," *Aerospace and Electronic Systems, IEEE Transactions on*, 1966.
[4] L. Campbell, "Sampling theorem for the Fourier transform of a distribution with bounded support," *SIAM Journal on Applied Mathematics*, vol. 16, 1968.
[5] J. Brown, "Bounds for truncation error in sampling expansions of band-limited signals," *Information Theory*, vol. 15, 1969.
[6] ——, "Truncation error for band-limited random processes," *Information Sciences*, vol. 1, 1969.
[7] P. Butzer and W. Splettstosser, "A sampling theorem for duration-limited functions with error estimates," *Information and Control*, vol. 34, 1977.
[8] Z. Xu, B. Huang, and X. Li, "On Fourier interpolation error for band-limited signals," *Signal Processing, IEEE Transactions on*, vol. 57, 2009.
[9] L. Moisan, "Periodic plus smooth image decomposition," *Journal of Mathematical Imaging and Vision*, vol. 39, 2011.
[10] G. Strang and G. Fix, "A Fourier analysis of the finite element variational method," *Constructive aspects of functional analysis*, 2011.
[11] T. Blu and M. Unser, "Quantitative fourier analysis of approximation techniques. i. interpolators and projectors," *Signal Processing, IEEE Transactions on*, vol. 47, 1999.
[12] L. Condat, T. Blu, and M. Unser, "Beyond interpolation: Optimal reconstruction by quasi-interpolation," *International Conference on Image Processing*, vol. 1, pp. I–33, 2005.